

RA1255

APR 25 1946

NATIONAL ADVISORY COMMITTEE  
FOR AERONAUTICS

TECHNICAL NOTE

No. 1038

STRUCTURAL HINGE-MOMENT INCREMENTS  
CAUSED BY HINGE-AXIS DISTORTION

By John V. Becker and Morton Cooper

Langley Memorial Aeronautical Laboratory  
Langley Field, Va.



Washington  
April 1946

N A C A LIBRARY  
LANGLEY MEMORIAL AERONAUTICAL  
LABORATORY

Langley Field, Va.



## NATIONAL ADVISORY COMMITTEE FOR AERONAUTICS

TECHNICAL NOTE NO. 1038

## STRUCTURAL HINGE-MOMENT INCREMENTS

CAUSED BY HINGE-AXIS DISTORTION

By John V. Becker and Morton Cooper

## SUMMARY

An investigation of elevators having three hinges has been made to evaluate the structural hinge-moment increments resulting from changing the elevator angle when the hinge axis is distorted under load. An equation is derived relating the structural hinge-moment increment to the elevator angle, to the structural stiffness factors of the elevator and stabilizer, and to the amount of hinge-axis distortion. The analytical results are compared with test data obtained for a full-scale semispan fighter-type horizontal tail surface in the Langley 16-foot high-speed tunnel. It is shown that the structural hinge-moment increments increase the control forces required to produce given elevator deflections. For large tail loads the structural hinge-moment increments are an appreciable fraction of the total hinge moment.

## INTRODUCTION

During an investigation in the Langley 16-foot high-speed tunnel of the aerodynamic characteristics of a full-scale semispan fighter-type production horizontal tail surface having three hinges, tests were made to evaluate possible effects of friction at the hinges on the accuracy of the hinge-moment data. Although the friction effects were found to be negligible, a systematic variation of hinge moment with elevator angle was found to occur when the tail was deflected under static load. This hinge moment was associated with distortion of the hinge axis and the resulting misalignment of the

hinges. When the elevator angle was varied with the hinges misaligned, deformations of both the elevator and the stabilizer structure occurred. The application of an appreciable structural hinge moment was required to deflect the elevator under these conditions.

The purpose of this paper is to present an analysis that permits the approximate calculation of the structural hinge-moment increments from a knowledge of the structural characteristics of the tail. The results of this analysis are compared with the structural hinge-moment increments measured on a full-scale tail. In order to illustrate the magnitude of the structural hinge-moment increments, a comparison is made of the corrected aerodynamic hinge-moment coefficients with the hinge-moment coefficients indicated in wind-tunnel tests of the full-scale tail.

Although the present analysis refers specifically to horizontal tails, it may be applied also to wing-aileron and fin-rudder combinations.

#### SYMBOLS

H	hinge moment
$\rho$	free-air density
$\rho_0$	sea-level density under standard conditions (0.002378 slugs/cu ft)
V	free airspeed
$V_i$	indicated airspeed $\left( V \sqrt{\frac{\rho}{\rho_0}} \right)$
q	dynamic pressure $\left( \frac{1}{2} \rho V^2 \right)$
$\bar{c}_e$	root-mean-square of elevator chord behind hinge line
$b_e$	elevator span
$C_h$	hinge-moment coefficient $\left( \frac{H}{q \bar{c}_e^2 b_e} \right)$

- $E_c$  chordwise stiffness factor of elevator measured at central hinge relative to end hinges, pounds per inch.
- $S_c$  chordwise stiffness factor of stabilizer measured at central hinge relative to end hinges, pounds per inch.
- $E_n$  normal-to-chord stiffness factor of elevator measured at central hinge relative to end hinges, pounds per inch.
- $S_n$  normal-to-chord stiffness factor of stabilizer measured at central hinge relative to end hinges, pounds per inch.
- $\delta$  angle of elevator chord with respect to stabilizer chord ( $\delta$  positive for trailing edge down)
- $d_0$  perpendicular distance from central hinge to line joining end hinges; elevator neutral ( $\delta = 0^\circ$ )
- $d$  perpendicular distance from central hinge to line joining end hinges; elevator deflected ( $\delta \neq 0^\circ$ )
- $\phi$  angle of rotation of central hinge about line joining end hinges (fig. 1)

## ANALYSIS

When a horizontal tail surface is deflected by lift loads, the hinge axis is not a straight line if more than two hinges are used (fig. 1). As the elevator angle is changed, the central hinge tends to be rotated eccentrically about a line through the end hinges. If the control moment is assumed to be applied at the inboard hinge, a hinge moment is introduced at this point by the force acting at the central hinge. This force is the sum of the aerodynamic load carried by the central hinge and the structural force resulting from resistance of the central hinge to the deformation introduced when the elevator is deflected. The hinge-moment increment that results from hinge-axis distortion thus consists of two components, one aerodynamic and one structural. Because the chordwise deformation of the hinge axis is ordinarily

extremely small, the hinge-moment increment caused by the aerodynamic lift on the elevator is usually negligibly small; hence, only the hinge-moment increment arising from the structural forces is considered in the present study.

It is assumed that the basic vertical misalignment of the central hinge  $d_0$  (fig. 1) is known from calculation of the deflection curve of the tail for the lift load condition being investigated. The total aerodynamic load used in calculating  $d_0$  should of course include the load carried by the deflected elevator. The moments of inertia used in evaluating  $d_0$ , however, should correspond to the elevator-neutral configuration. The quantity  $d_0$  is thus the vertical displacement of the central hinge that would occur if the actual tail load (elevator deflected) were applied to the tail with elevator neutral. The structural hinge moment for the elevator-neutral condition is assumed to be zero for all values of  $d_0$ . Beyond the determination of  $d_0$  no further consideration need be given to the air load. For simplicity, the elevator may be visualized as carrying no air load since only the structural hinge-moment increments due to hinge-axis distortion are to be evaluated.

From the schematic representation of the deflected elevator with distorted hinge axis (fig. 1), the following relationships can be determined:

$$\text{Chordwise deflection of central hinge relative to undeformed elevator, } \frac{d \sin (\delta - \phi)}{\cos \phi}$$

$$\text{Normal deflection of central hinge relative to undeformed elevator, } \frac{d \cos (\delta - \phi)}{\cos \phi}$$

$$\text{Chordwise force, } E_c \frac{d \sin (\delta - \phi)}{\cos \phi}$$

$$\text{Normal force, } E_n \frac{d \cos (\delta - \phi)}{\cos \phi}$$

The structural hinge moment induced as a result of the deflection of the central hinge is given by the sum of the individual moments of the chordwise and normal-to-chord forces about the axis through the inboard and outboard

hinges about which the control moment is assumed to act. Thus,

$$H = E_c \frac{d \sin(\delta - \phi)}{\cos \phi} - E_n \frac{d \cos(\delta - \phi)}{\cos \phi}$$

or

$$\frac{H}{d_0^2 (E_c - E_n)} = \frac{1}{2} \left( \frac{d}{d_0} \right)^2 \frac{\sin 2(\delta - \phi)}{\cos \phi} \quad (1)$$

In accordance with the aerodynamic sign convention, this parameter  $\frac{H}{d_0^2 (E_c - E_n)}$  is negative for positive elevator angles and is positive for negative elevator angles.

Equation (1) expresses the structural hinge moment as a dimensionless parameter that is a function of the physical properties of the tail, the elevator angle, and the distortion of the hinge line. In order to evaluate the parameter  $\frac{H}{d_0^2 (E_c - E_n)}$ , the angle  $\phi$  and the ratio  $d/d_0$  must first be determined in terms of the known stiffness factors and elevator angle. From the equilibrium condition in a direction parallel to the stabilizer chord,  $\phi$  is determined by

$$S_c d \tan \phi = E_c \frac{d \sin(\delta - \phi) \cos \delta}{\cos \phi} - E_n \frac{d \cos(\delta - \phi) \sin \delta}{\cos \phi}$$

or

$$\phi = \tan^{-1} \left[ \frac{\frac{1}{2} \left( \frac{E_c}{E_n} - 1 \right) \sin 2\delta}{\frac{E_c + S_c}{E_n} - \left( \frac{E_c}{E_n} - 1 \right) \sin^2 \delta} \right] \quad (2)$$

From the condition of equilibrium in a direction normal to the stabilizer chord,  $d/d_0$  is evaluated as follows:

$$S_n(d_0 - d) = E_c \frac{d \sin(\delta - \phi) \sin \delta}{\cos \phi} - E_n \left( d_0 - \frac{d \cos(\delta - \phi) \cos \delta}{\cos \phi} \right)$$

or

$$\frac{d}{d_0} = \frac{\frac{S_n}{E_n} + 1}{\left( \frac{E_c}{E_n} - 1 \right) \left( \sin^2 \delta - \frac{1}{2} \sin 2\delta \tan \phi \right) + \left( \frac{S_n}{E_n} + 1 \right)} \quad (3)$$

Figure 2 presents a plot of the structural hinge-moment parameter  $\frac{H}{d_0^2 (E_c - E_n)}$  against  $\delta$  for representative

values of  $E_c/E_n$  and  $S_c/E_c$ . The two values,  $\frac{E_c}{E_n} = 15$  and  $\frac{E_c}{E_n} = 10$ , for which the curves of figure 2 were prepared were the approximate values measured for two full-scale fighter-type tails. In preparing figure 2, the ratio of chordwise to normal stiffness for the stabilizer was taken as equal to this ratio for the elevator; that is,  $\frac{E_c}{E_n} = \frac{S_c}{S_n}$ . These ratios were found experimentally to be approximately equal for a fighter-type tail

as is shown subsequently in the section entitled "Determination of Structural Stiffness Factors." Figure 2 shows that the effect of reducing  $E_c/E_n$  is similar to increasing  $S_c/E_c$ . The upper-limit curve of  $S_c/E_c$  in figure 2 represents an infinitely rigid stabilizer having an initial set  $d_0$ , in which case the structural hinge-moment parameter (equation (1)) simplifies to

$$\frac{H}{d_0^2(E_c - E_n)} = \frac{1}{2} \sin 2\delta. \quad \text{Figure 2 also shows that, for}$$

a fixed value of  $d_0$  (approx. fixed tail load), the structural hinge moments for tails having  $S_c/E_c$  values from about 3 to 10 reach a maximum at elevator angles in the range  $20^\circ$  to  $30^\circ$ . Values of  $S_c/E_c$  in this range are believed to be representative of current construction. The effects of a change in the value of  $E_c/E_n$  from 10 to 15 are negligible at high values of  $S_c/E_c$  but of appreciable magnitude at the lower values of  $S_c/E_c$ .

Inasmuch as the dimensionless hinge-moment parameter  $\frac{H}{d_0^2(E_c - E_n)}$  involves the square of the vertical mis-

alignment  $d_0$ , the structural hinge moment  $H$  increases as the square of the vertical misalignment for a given elevator and elevator angle. In addition, since  $d_0$  is approximately a linear function of the total tail lift load, the structural hinge moment therefore varies approximately as the square of the tail lift load.

From equations (1), (2), and (3), the difference between chordwise and normal stiffness factors can be shown to have a significant effect on the structural hinge moment. Because the chordwise stiffness factors are considerably larger than the normal stiffness factors, it is evident that appreciable reductions in structural hinge moment would result from reducing the chordwise stiffness factors. This reduction might be accomplished by mounting the central hinge bracket to permit a limited degree of freedom in the chordwise plane.

The analysis as presented can be adapted to stabilizer-elevator, wing-aileron, and fin-rudder combinations having three hinges located as shown in figure 1. The results may also be applied if the inboard hinge is located on

the center line of the airplane and is a common hinge for both tail surfaces. If each of the two tail surfaces contains three hinges and is attached to the other by a carry-over assembly through the center line of the airplane, the accuracy of the results obtained by this analysis would depend upon the flexibility of the carry-over assembly. The torque-tube assembly in the carry-over region usually has only a small fraction of the chordwise stiffness of the elevator, and therefore the analysis is considered valid as a first approximation for this type of installation.

#### DETERMINATION OF STRUCTURAL STIFFNESS FACTORS

The use of the foregoing analysis to estimate the structural hinge-moment increments requires a knowledge of the chordwise and normal-to-chord stiffness factors of both the stabilizer and the elevator. These factors usually involve not only the stiffness of the primary structure and the skin but also, to a large extent, the stiffness of attachment of the hinge brackets. It is obvious, therefore, that these factors should be determined experimentally. For either the stabilizer or the elevator the factors may be easily determined by supporting the surface at the end hinges and applying loads at the central hinge in both the chordwise and normal-to-chord planes and by measuring the corresponding deflections at the central hinge.

In addition to the stiffness factors, the analysis requires a knowledge of the misalignment  $d_0$  of the central hinge with respect to a straight line through the inboard and outboard hinges for the elevator-neutral condition. This value can be easily determined from the elastic deflection curve of the tail surface. As previously discussed, the moments of inertia used in the calculations should correspond to the elevator-neutral setting, but the lift loads used should be those for the actual design configuration being investigated.

Stiffness factors have been measured for two typical production fighter-type horizontal tail surfaces. Tail 1, shown in figure 3, has a 30-percent-chord internally-balanced elevator and was designed for a 12,000-pound jet-propelled airplane. Tail 2, figure 4, has a 28-percent-chord elevator with an exposed overhang type of aerodynamic

balance and was designed for a 24,000-pound jet-propelled airplane. The stiffness factors for the stabilizer of tail 2 were not obtained. The following table shows the stiffness factors measured for the two tails:

Tail	$E_c$	$S_c$	$E_n$	$S_n$
1	6,300	17,900	580	1,735
2	14,300	-----	950	-----

The stiffness-factor ratios for comparison with those used in preparing figure 2 are:

Tail	$E_c/E_n$	$S_c/S_n$	$S_c/E_c$	$S_n/E_n$
1	10.86	10.32	2.84	2.99
2 <sup>a</sup>	15.05	-----	<sup>a</sup> / <sub>6</sub>	<sup>a</sup> / <sub>6</sub>

<sup>a</sup>Estimated from comparison of measured structural hinge moments with analytical results shown in figure 2.

The ratio  $S_c/S_n$  is closely equal to  $E_c/E_n$  (see preceding table) as assumed in the preparation of figure 2.

#### COMPARISON OF CALCULATED AND MEASURED STRUCTURAL HINGE MOMENTS

The variation of structural hinge moment with elevator angle was measured for tail 1 (fig. 3). The stabilizer semispan was loaded statically with 1200 pounds varying along the span as a linear function of the chord. The elevator angles and hinge moments were measured with the tail deflected under this load. The deflection curve of the tail with elevator neutral was determined at the hinge axis. The chordwise and normal stiffness factors of the elevator and stabilizer were determined by mounting the elevator and stabilizer individually on their end.

hinge brackets and by applying a load at the central hinge. The measured stiffness factors corresponded to the condition of positive elevator deflections with a net down load on the tail.

By use of the measured stiffness factors for the positive elevator angles, structural hinge moments were calculated from equations (1), (2), and (3). The calculated results are compared with the experimentally determined structural hinge moments in figure 5. The agreement for positive elevator angles is considered satisfactory. For negative elevator angles, the apparent discrepancy of about 20 percent is taken to indicate that the stiffness factors for positive deflections which were used in the calculations differed appreciably from those for negative deflections. Unfortunately this result was not discovered in time to permit measurement of the stiffness factors for negative elevator angles. The trend of the experimental curve for negative angles agrees well with the calculated curve in spite of the 20-percent discrepancy in the values of the calculated hinge moment.

The peak value of the structural hinge moment was about 25 inch-pounds for the test tail semispan load of 1200 pounds. For the design semispan load of 3900 pounds, the structural hinge moment would be approximately

$$25 \left( \frac{3900}{1200} \right)^2 \text{ or } 264 \text{ inch-pounds.}$$

#### COMPARISON OF STRUCTURAL HINGE-MOMENT

#### INCREMENTS WITH AERODYNAMIC HINGE MOMENTS

In order to compare the magnitude of the structural hinge-moment increments with values of the aerodynamic hinge moments, structural hinge-moment increments for tail 2 (fig. 4) were reduced to hinge-moment coefficient form for a representative indicated airspeed of 316 miles per hour. Aerodynamic data for the tail surface obtained from tests in the Langley 16-foot high-speed tunnel were used to compute the loads and the corresponding hinge-line deflections for a range of angles of attack.

and elevator angles. Figure 6 presents the wind-tunnel hinge-moment data for the tail and, for comparison, the corrected aerodynamic data (wind-tunnel hinge-moment data minus structural hinge-moment increments). Since for a given tail and elevator angle the magnitude of the structural hinge moment is dependent only on the load on the tail, lines of constant load have been superimposed on the hinge-moment-coefficient curves of figure 6 to show the effect of load on the structural hinge-moment increments. The design load of the semispan tail tested was about 8500 pounds. The structural hinge-moment increments are an appreciable part of the total measured hinge moment at large tail loads and at high elevator deflections. The effect of the increments is to increase the control forces required to produce a given elevator deflection.

### CONCLUSIONS

An investigation of elevators having three hinges has been made to evaluate the structural hinge-moment increments resulting from changing the elevator angle when the hinge axis is distorted under load and indicates the following conclusions:

1. The structural hinge-moment increments can be calculated from the analysis presented in this report provided the following structural characteristics are known:

(a) The normal-to-chord and chordwise stiffness factors of elevator and stabilizer measured at the central hinge with respect to the end hinges

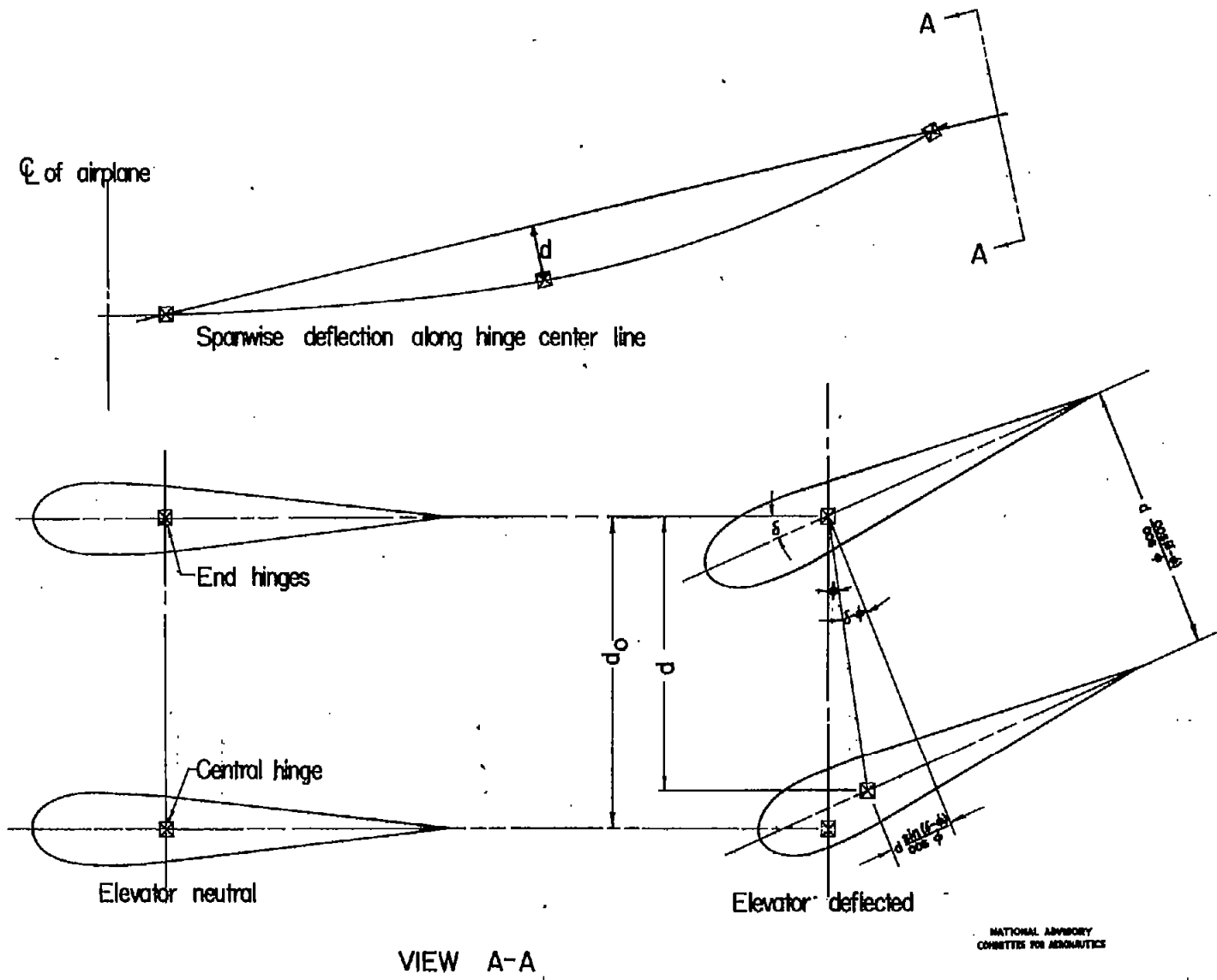
(b) The elastic deflection curve of the tail surface with elevator neutral for the lift load condition being investigated

2. For a given misalignment of the hinges the structural hinge-moment increments increase indefinitely as the elevator chordwise stiffness factor is increased. Appreciable reductions in the structural hinge-moment increment can be effected by reducing the chordwise stiffness factor.

3. The structural hinge-moment increment for a fixed elevator angle varies approximately as the square of the lift load on the tail. For a fixed tail load condition, the structural hinge-moment increments increase with increasing elevator angle until a maximum value is reached at elevator angles in the range of  $20^{\circ}$  to  $30^{\circ}$ .

4. The structural hinge-moment increments for a full-scale fighter-type horizontal tail surface tested in the Langley 16-foot high-speed tunnel appreciably increased the control forces required to produce a given elevator deflection at large tail loads and high elevator angles.

Langley Memorial Aeronautical Laboratory  
National Advisory Committee for Aeronautics  
Langley Field, Va., December 13, 1945



NATIONAL ADVISORY  
COMMITTEE FOR AERONAUTICS

FIGURE 1.— SCHEMATIC REPRESENTATION OF ELEVATOR WITH DISTORTED HINGE AXIS.

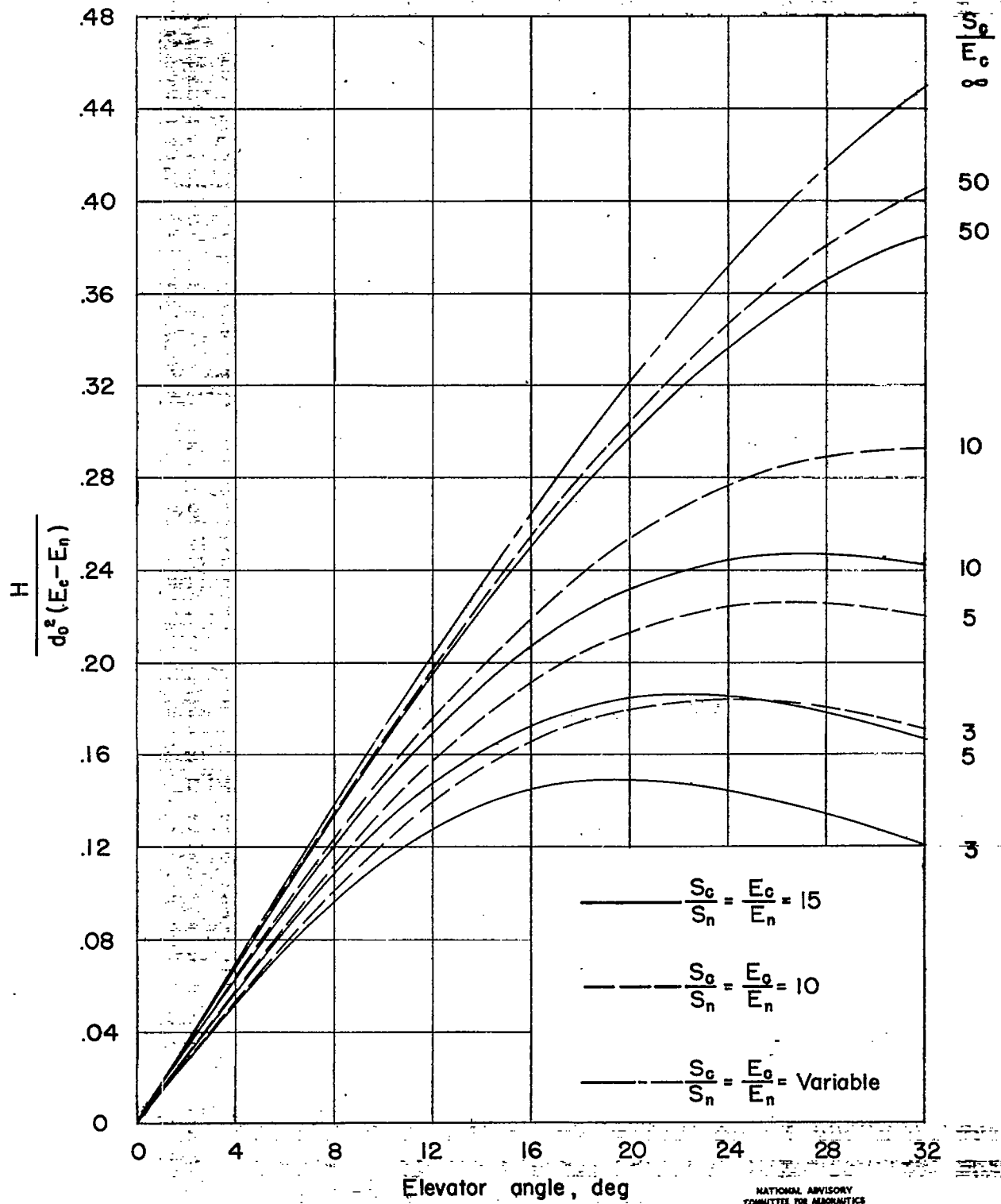
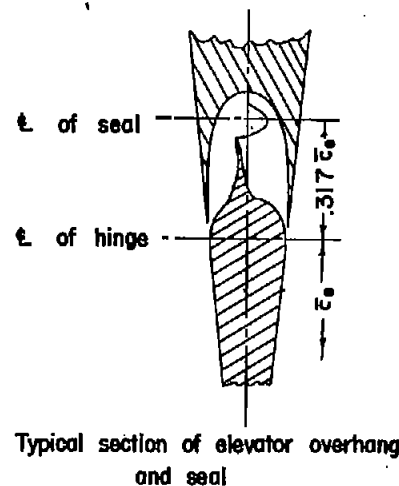
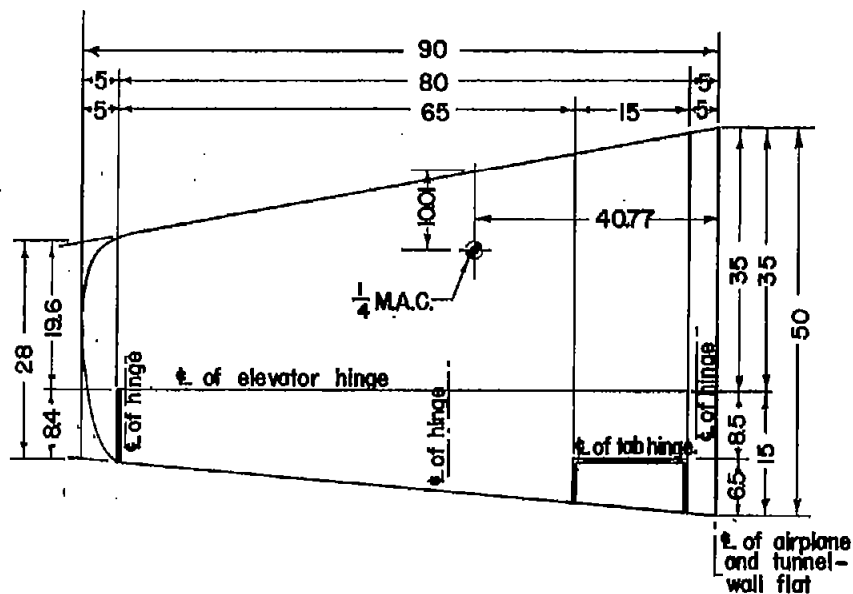


Figure 2.— Variation of dimensionless hinge-moment parameter with elevator angle for representative elevator-stabilizer stiffness combinations.

NATIONAL ADVISORY  
COMMITTEE FOR AERONAUTICS

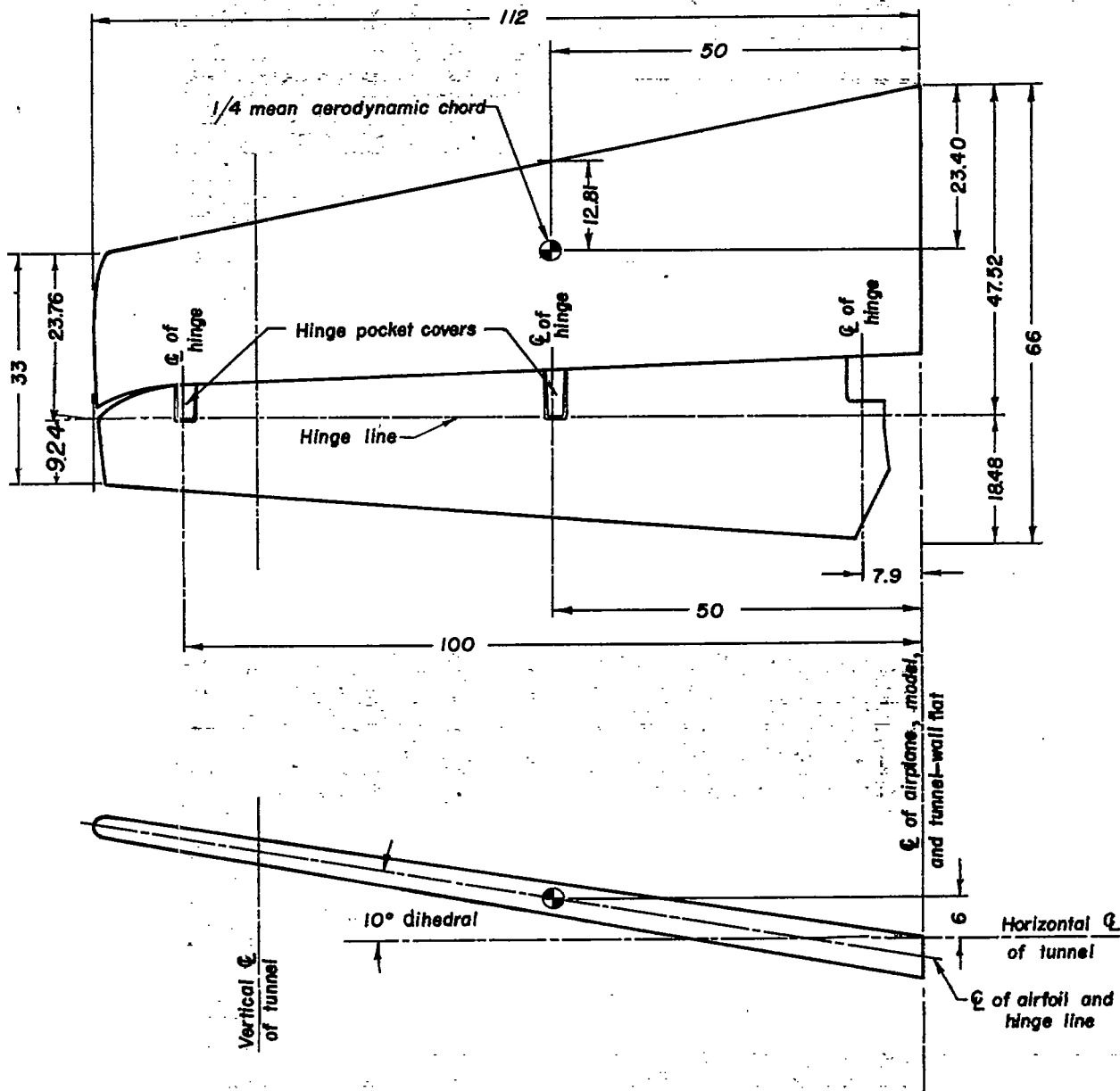


Tail dihedral, deg .....	5
Thickness ratio, percent .....	10
Root-mean-square of elevator chord behind hinge line, in. ....	11.70
Mean aerodynamic chord, in. ....	40.04
Stabilizer area, sq in. ....	2184
Elevator area, sq in. ....	1233

Figure 3.—General arrangement of horizontal tail surface 1.

(All dimensions in in. and measured in plane of section)

NATIONAL ADVISORY  
COMMITTEE FOR AERONAUTICS



Root-mean-square of elevator chord behind hinge line, in.....	13.74
Mean aerodynamic chord, in.....	51.3
Stabilizer area, sq in.....	3259.0
Elevator area, sq in.....	1429.0
Overhang area, sq in.....	596.0

NATIONAL ADVISORY  
COMMITTEE FOR AERONAUTICS

Figure 4.—General arrangement of horizontal tail surface 2 in Langley 16-foot high-speed tunnel. (All dimensions in in. and measured in plane of section.)

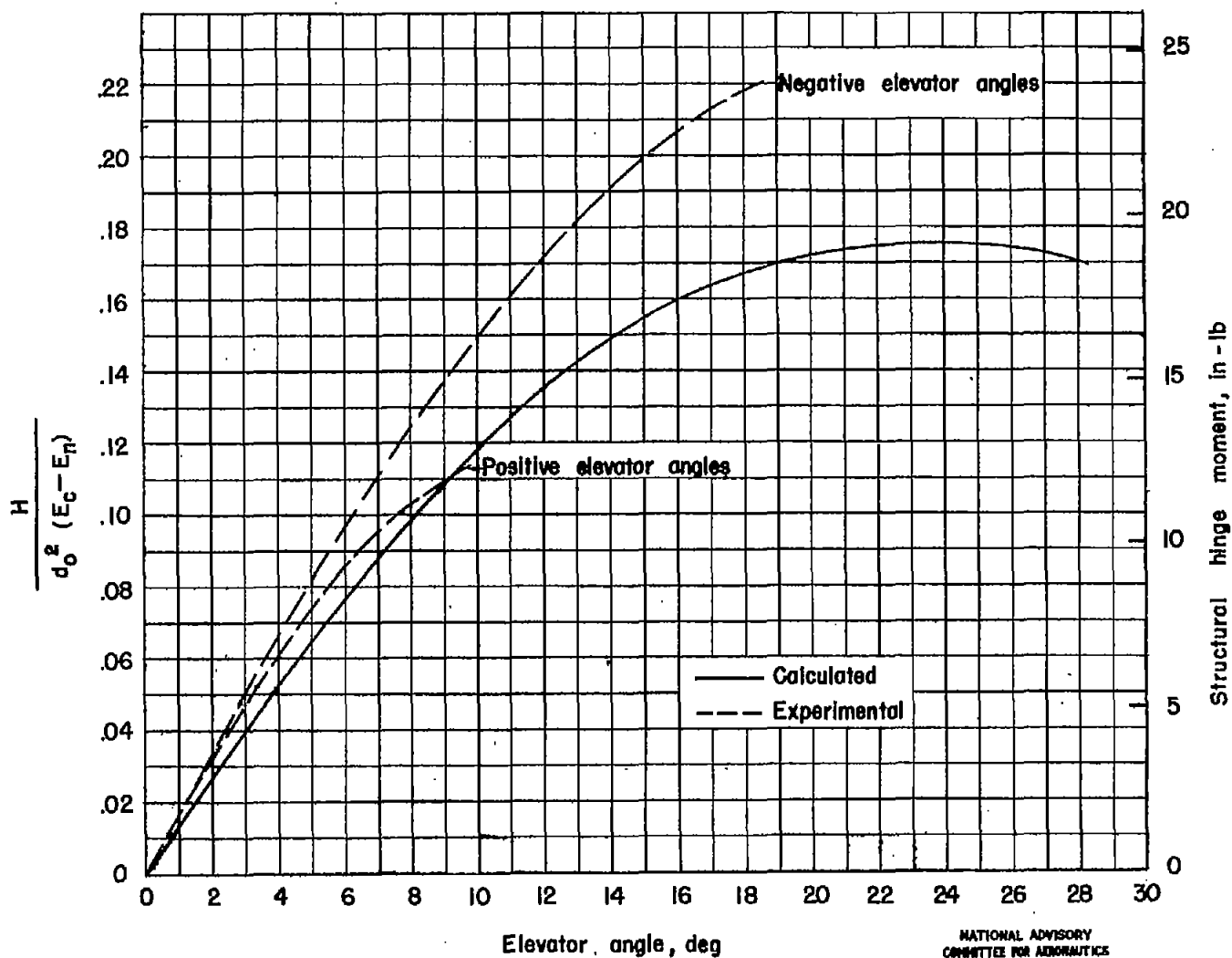


Figure 5.—Comparison of calculated and experimentally determined structural hinge moments for tail 1.  $d_0=0.138$  inch; tail load =1200 pounds.

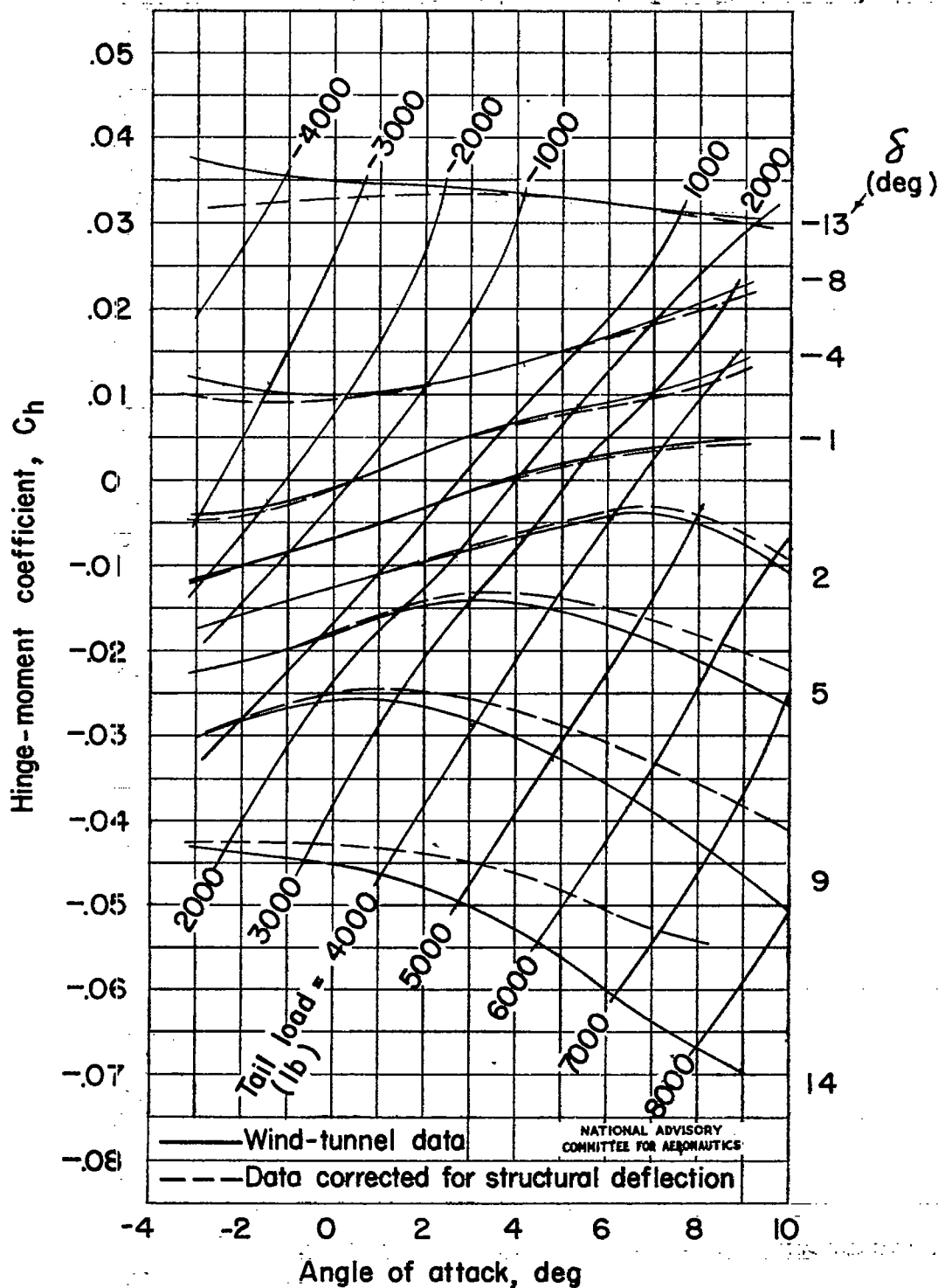


Figure 6.—Effect of structural deflections on hinge-moment coefficient; tail 2 ;  $V_i = 318$  miles per hour.